North Brazil Current retroflection and transports

Silvia L. Garzoli,[1] Amy Ffield,[2] William E. Johns,[3] and Qi Yao[4]

Received 9 January 2003; revised 7 July 2003; accepted 12 September 2003; published 17 January 2004.

[1] A subset of data collected as a part of a larger program, the North Brazil Current Rings (NBCR) Experiment, is analyzed to study the variability of the transport of the North Brazil Current (NBC) and its relation with the shedding of rings. It is concluded that there is a direct relation between the latitude of penetration, the number of rings shed, and the intensity of the NBC. The data set consists of dynamic height time series derived from three inverted echo sounders and a shallow pressure gauge deployed along a section perpendicular to the South American coast between the continent and 7°N, and between 48° and 45°W. Velocity and hydrographic data collected during the NBCR cruises are also analyzed and used to validate the results. The 15-month mean transport of the NBC is 16 ± 2 Sv. The 18-month mean of the retroflected southeastward flow is 22 ± 2 Sv. Both flows display considerable variability. The retroflected southeast flow reaches its maximum value during September 1999, near the time when the climatological North Equatorial Countercurrent (NECC) reaches its maximum strength and it is minimum when the climatological NECC reverses or is not present in the basin. The mean difference between the NBC flow and the retroflected flow during August–December 1999 when the NECC is fully established is −7 Sv. The excess in the retroflected flow is due to North Atlantic water joining the retroflected flow from the South Atlantic. The combination of both flows constitutes the NECC. *INDEX TERMS:* 4576 Oceanography: Physical: Western boundary currents; 4520 Oceanography: Physical: Eddies and mesoscale processes; 4231 Oceanography: General: Equatorial oceanography; *KEYWORDS:* North Brazil Current, meridional overturning circulation, interhemispheric exchanges

Citation: Garzoli, S. L., A. Ffield, W. E. Johns, and Q. Yao (2004), North Brazil Current retroflection and transports, *J. Geophys. Res.*, *109*, C01013, doi:10.1029/2003JC001775.

1. Introduction

[2] The Atlantic Ocean is unique because of its role in the net transport of heat northward across the equator. This is due to the meridional overturning circulation (MOC) where cold, dense North Atlantic Deep Water is convectively formed at high latitudes and exported southward across the equator into the southern oceans. Most of this water eventually leaves the Atlantic basin and is replaced by warm water that flows northward from the South Atlantic across the equator. The Benguela Current, which flows northward as the eastern part of the South Atlantic subtropical gyre, carries the upper limb of the MOC to the western side of the basin. The flow is mainly confined between 22° and 35°S, and the transport of intermediate water is estimated to be 15 ± 2 Sv (sverdrup, 1 Sv = 1 × 10^{-6} m^3/s) [*Richardson and Garzoli*, 2003]. After that, the flow cannot follow a simple path due to wind-driven gyres that present obstacles. This is particularly valid when upper limb of the MOC reaches the tropics where equatorial upwelling, off-equatorial downwelling, Intertropical Convergence Zone (ITCZ) induced motions, subtropical cells circulation, and the strong seasonal cycle of the wind-driven gyres hinder the upper limb of the MOC moving from the South Atlantic to the North Atlantic.

[3] Currently, there is not enough observational evidence to trace the pathways of the upper limb across the tropics. Most of our knowledge comes from modeling studies. A recent study [*Fratantoni et al.*, 2000] uses an eddy-resolving numerical oceanic circulation model to investigate the pathways of low-latitude intergyre mass transport associated with the upper limb of the Atlantic MOC. *Fratantoni et al.* [2000] concluded that the 14-Sv upper ocean MOC return flow is partitioned among three pathways connecting the equatorial and tropical wind-driven gyres: a frictional western boundary current that accounts for 6.8 Sv of intergyre transport, a diapycnal pathway involving wind-forced equatorial upwelling and interior Ekman transport that is responsible for 4.2 Sv, and North Brazil Current (NBC) rings shed at the retroflection that contribute approximately 3.0 Sv of intergyre transport. Most of the observational studies [e.g., *Johns et al.*, 1990, 1998; *Stramma et al.*, 1995; *Schott et al.*,

[1]Atlantic Oceanographic and Meteorological Laboratory, National Oceanic and Atmospheric Administration, Miami, Florida, USA.
[2]Lamont-Doherty Earth Observatory of Columbia University, Palisades, New York, USA.
[3]Rosenstiel School of Marine and Atmospheric Sciences, University of Miami, Miami, Florida, USA.
[4]Cooperative Institute for Marine and Atmospheric Studies, Miami, Florida, USA.

0148-0227/04/2003JC001775

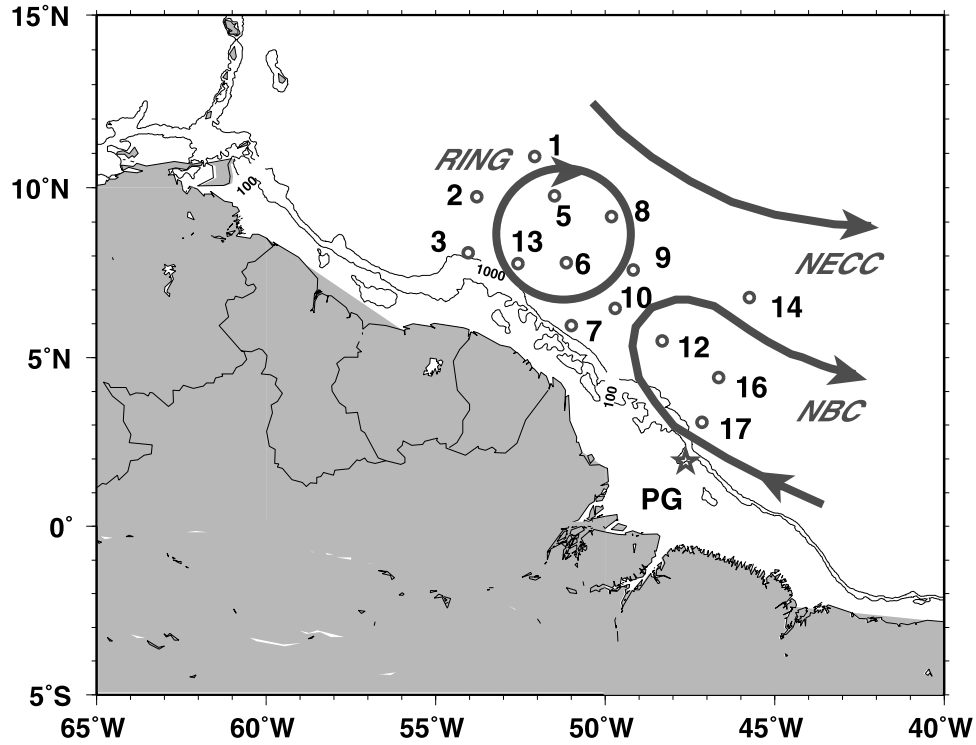

Figure 1. Map of the area of the NBCR experiment. The circles indicate the location of the moored inverted echo sounders (IES) and the star indicates the location of the pressure gauge (PG). Red arrows are a schematic of the mean currents (NBC and NECC), the location of the mean NBC retroflection, and the rings shed.

1995; *Bourles et al.*, 1999a] suggested that NBC is one of the major contributors to the interocean exchange of heat and mass.

[4] The NBC is the western boundary current of the wind-driven gyre in the northern tropical Atlantic. At its retroflection, rings are shed, resulting in a significant transfer of mass and heat. Previous results based on satellite images as well as in situ observations indicated an average of two to four rings shed at the retroflection per year [i.e., *Didden and Schott*, 1993; *Johns et al.*, 1990; *Richardson et al.*, 1994]. On the basis of these estimates, it was suggested that typically these rings might account for one third (approximately 3 Sv) of the total upper transport in the warm limb of the Atlantic MOC. Nonetheless, observations still suggest that a component of the NBC flows directly to the Caribbean by way of a more-or-less steady current: (1) northwestward along shore flows of 10 and 12 Sv were observed in March 1994 and in March 1996 [*Schott et al.*, 1998]; (2) a 3–5 Sv annual flow was inferred over the continental shelf in 1989–1991 [*Johns et al.*, 1998]; and (3) further upstream, in March 1994 and April 1996 a 7-Sv flow was observed [*Bourles et al.*, 1999a].

[5] Averaging the above steady current and translating ring estimates, the combined volume transport for the direct NBC to Caribbean route is on the order of 8 Sv/yr or about half of the volume flow needed to complete the upper interhemispheric loop. In addition, there might be a contribution from sporadic filaments of the NBC, as found in the Agulhas retroflection south of Africa [*Garzoli and Gordon*, 1996; *Garzoli et al.*, 1996]; these would not have the consolidated flow properties of the rings, but they would still contribute to the volume flow. Presumably, the remaining half of the interhemispheric flow can come from the indirect route, by way of the equatorial recirculation cells.

[6] In order to study the NBC and the processes of rings shedding at the retroflection, an intensive multiinstitutional program was carried out called the North Brazil Current Rings (NBCR) experiment. As part of this program, an array of 14 inverted echo sounders (IES) was deployed in the region of the retroflection and ring formation (Figure 1). The main objective of the array was to provide a three-dimensional (time/space) field of the dynamic height to study the NBC variability and the related eddy field. In particular, the array was designed (1) to monitor the poleward displacement of the front associated with the retroflection of the North Brazil Current (retroflection front), (2) to monitor the passage of rings and study the process of eddy formation and propagation, (3) to provide an estimate of the strength of the NBC transport and the offshore retroflected flow, and (4) to determine the relationship of the NBC transport to the number of rings shed.

[7] In a recent publication [*Garzoli et al.*, 2003] the array of IES was analyzed to determine from synoptic maps of dynamic height, the variability of the latitude of retroflection and the number of rings shed during the experiment. Results from this analysis indicated that there is no apparent seasonality on the northwestern location of the penetration and that almost every time that the retroflection increases its northwest penetration, a ring is shed. During the total period of time covered by the observations (November 1998 to

Table 1. Instrument Locations and Dates

Site	Deployment	Latitude	Longitude	Depth, m	Recovery
Pressure gauge	March 5, 1999	01°54.58′N	47°38.22′W	68	June 9, 2000
IES 17	November 23, 1998	03°04.70′N	47°09.05′W	1802	June 9, 2000
IES 16	November 23, 1998	04°24.89′N	46°39.18′W	3273	June 10, 2000
IES 14	November 22, 1998	06°46.01′N	45°44.60′W	4200	June 10, 2000

June 2000) a total of 11 rings was shed. The rings transported in the mean 7–9 Sv of water and 0.6 PW of heat. These estimates indicate that the contribution of the rings to the interhemispheric exchange of heat is considerably larger than previous estimates. Recent observations indicated that the number of rings shed at the retroflection were five to six rings per year from altimeter-derived sea height anomaly data [*Goni and Johns*, 2001] and six rings per year (total ~6 Sv/yr) from ocean color derived chlorophyll data [*Fratantoni and Glickson*, 2002]. Both estimates are lower than those provided as the result of the analysis of NBCR data [*Garzoli et al.*, 2003; *Goni and Johns*, 2003; *Johns et al.*, 2003]. There is also an indication of interannual variability in the latitude of penetration in the mid-November to May time period: the latitude of penetration was further north and more rings were shed in 1998/1999 than in 1999/2000 [*Garzoli et al.*, 2003].

[8] In this paper, a subset of data collected as part of the NBCR experiment just southeast of the NBC retroflection and ring shedding region is analyzed to further study the variability of the NBC transport, the southeastward retroflected flow transport in the offshore part of the retroflection, and their relation to ring shedding and the latitude of penetration.

2. The Data

[9] Three of the IES deployed as part of the larger array were moored along a section perpendicular to the South American coast between the continent and 7°N and between 48° and 45°W. The site of the deployments was chosen to obtain an estimate of the strength of the NBC transport (Figure 1, IES 14 to 17) and the retroflected flow. During the first cruise (NBCR 1, 7 November to 11 December, 1998) it became evident from acoustic Doppler current profiler (ADCP) observations that these three sites did not capture a large part of the northwestern flow. During the second cruise (NBCR 2, February 1999) a pressure gauge (PG) was deployed to capture the missing flow between site IES 17 and the coast. All the instruments recorded hourly averaged values, and they were securely anchored to the ocean floor. Their deployment and recovery information is listed in Table 1.

[10] Four research cruises took place during the experiment. ADCP velocity data were obtained from the near surface to 200 m during the ship transits of all four cruises. During the first three cruises, conductivity-temperature-depth-oxygen (CTD-O_2) hydrographic station data and lowered ADCP (LADCP) velocity station data were obtained in the water column from the surface to the bottom. Along the section line defined by the location of the four moored instruments listed in Table 1, 24 CTD-O_2/LADCP stations were occupied. The ADCP and LADCP velocity data were detided using a global model of ocean tides, TPXO.3 [*Egbert et al.*, 1994], and rotated to obtain the flow perpendicular to the section. The hydrography data will be used to calibrate the time series data collected by the moored instruments. Together, the hydrography and velocity data will be used (1) to describe the flow through the section, (2) to provide new estimates of the NBC transport, and (3) to validate the geostrophic transport time series determined from the moored instruments. To do this, the ADCP and LADCP data were combined, gridded, and interpolated along the section defined by the four moored instruments. The vertical resolution of the data was 10 m for the LADCP and 8 m for the ADCP. The most complete section including the shelf along the line of deployments was obtained during November 1998, and the combined ADCP and LADCP velocity section is shown in Figure 2 as an example. Additional CTD-O_2/LADCP stations were obtained northwest of the section as part of the experiment but they are not used in the present study.

2.1. Dynamic Height Series

[11] The IES measures the travel time (TT) between the ocean surface and the depth of the deployed instrument. Time series of travel time can be directly related to time series of thermocline depth, integrated temperature, and dynamic height [i.e., *Watts and Johns*, 1982; *Garzoli*, 1984; *Garzoli and Garraffo*, 1989; *Garzoli and Gordon*, 1996]. The methodology used to obtain dynamic height time series from travel time measured with the IES during the NBCR experiment is the same as in the work by *Garzoli et al.* [2003]. It was observed that different relationships held for the ring shedding area (west of 50°W) and for the NBC retroflection area (east of 50°W). The following relation was derived to obtain changes in dynamic height (D) from changes in TT in the NBC retroflection area (east of 50°W) [*Garzoli et al.*, 2003]:

$$\Delta D = -0.061\Delta\mathrm{TT} \pm 0.027\,\mathrm{dyn\ m}, \quad R^2 = 0.89 \qquad (1)$$

where ΔD and ΔTT are the relative changes of dynamic height and travel time (surface relative to 300 dbar), respectively. R^2 is the square of the correlation coefficient between the two variables. The standard error of the estimate is ±0.027 dyn m. From this relation, time series of relative changes in dynamic height were calculated for each of the three IES time series. During the NBCR cruises CTD stations were collected at each IES location for the purpose of calibration. Dynamic heights at the surface relative to 300 dbar (D_{300}) were calculated at these CTD stations. The D_{300} values were used to calibrate the dynamic height time variability (ΔD) time series into dynamic height time series by adding a value that represents the best fit between the IES and CTD data. In all cases this value was a simple

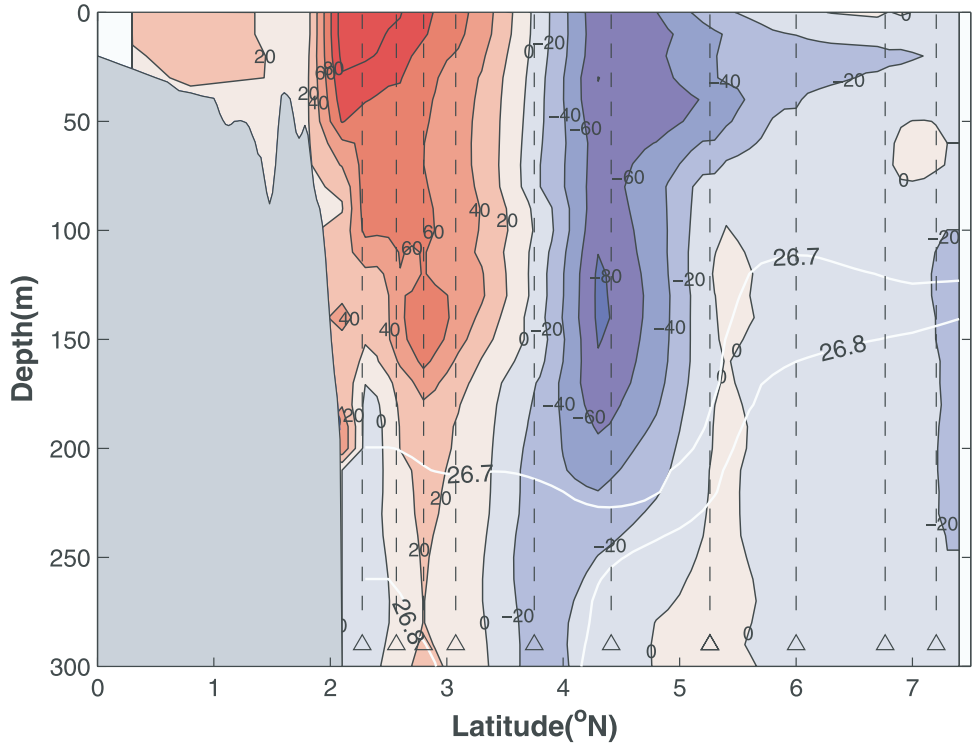

Figure 2. Velocities perpendicular to the line of deployments (PG to IES 14, see Figure 1) obtained as a composite of the data collected with the ADCP and LADCP during the first NBCR cruise in November 1998. Superimposed are the 26.8 and 26.7 isopycnals; triangles and dashed lines are the locations of the CTD/LADCP stations.

constant. The three series of D_{300} obtained by this method from the travel time collected with the IES and used in this publication are given in Figure 3. The reference level of 300 dbar was chosen from a review of the literature showing that the 26.8 isopycnal (which is shallower than 300 m) is generally used to define the lower boundary of the NBC and retroflected flow. This will allow comparison with earlier studies. In addition, the best correlation of the dynamic height with travel time was found with the 300-dbar reference level. The series shown in Figure 3 have been passed through a filter that eliminates periodicities less than 2 days. The series started in November 1998 and ended in June 2000. Circles indicate the dynamic height values calculated from the calibration CTD stations; they are shown for the purpose of comparison and to indicate the relatively small magnitude of the errors incurred with the calibration methodology. The actual values and the corresponding statistics are given in Table 2. The mean difference is 0.015 dyn m, with a standard deviation of 0.013 dyn m.

[12] A fourth time series of dynamic height was obtained from the PG record [*Garzoli et al.*, 2003]. The measured variations in bottom pressure (P) include three effects: (1) atmospheric pressure variations, (2) sea surface height variation, and (3) density changes in the shallow water column (baroclinic effects). The direct effects of atmospheric pressure variations are compensated by an inverse barometer response in the sea level, leaving only a dynamic signal related to sea level and baroclinic variations. What we desire from the PG is a proxy for the surface dynamic topography that can be compared with the corresponding records from the IES. If baroclinic effects over the shallow shelf region are neglected, the bottom pressure record is equivalent to the sea surface height variation and can be converted to a surface dynamic height by $dD = dP/\rho$, where ρ is the density of seawater. Signals due to baroclinic variations in the upper 68 m are not accounted for and therefore this is an approximation. The variability in dynamic height was obtained from the pressure time series (PG) in a similar way as for the IES (i.e., equation (1)). The difference resides in the absolute value of dynamic height. The PG was deployed at 68 m, and therefore to obtain a time series of dynamic height at the surface reference to 300 m, extrapolations are needed. Initially, the CTD casts at 68 m were extrapolated to 300 m using adjacent and historical data. As the errors by doing so were unknown, a second adjustment to the series was made to fit the values of velocities obtained with the ADCP during the three cruises. Methods for calibrating the dynamic height time series from the IES and PG records to obtain time series of upper ocean transport (0–300 m) are described in the next section. The time series of dynamic height from the pressure record is also shown in Figure 3. It must be noted that the pressure gauge record, as well as the travel time series collected further north on the shelf [*Garzoli et al.*, 2003], shows higher-frequency oscillations than the series collected offshore. The series obtained at the PG site started in February 1999 and ended on June 2000.

[13] There are two components to the error in dynamic height ($\varepsilon(D)$). The first one is the error in estimating ΔD

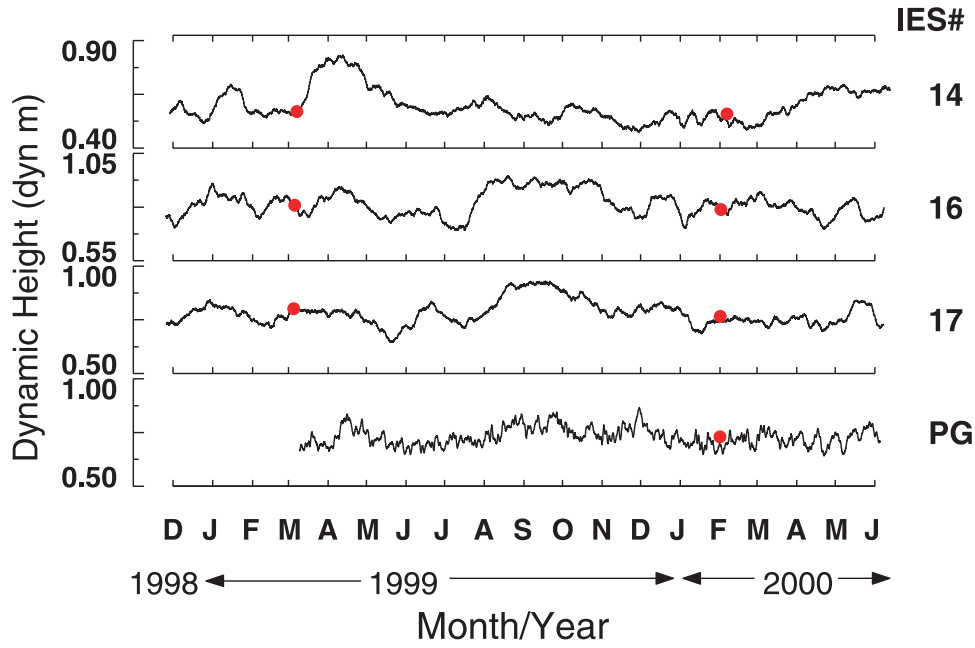

Figure 3. Time series of dynamic height at the surface, reference 300 m obtained from the observations collected at IES sites 17, 16, and 14 and with the PG. Red circles indicate the dynamic height value obtained from the CTD data collected at the time of the cruises (Table 2).

from ΔTT. This is the error of the regression (0.027 dyn m) and is the same for all series. The second one is the error adjusting the series of ΔD to absolute values (Table 2) and is different for each one of the station pairs. Therefore the total error varies for each series and is the sum of the two: It is 0.015 m/s for IES 14, 0.030 m/s for IES 16, 0.038 m/s for IES 17, and 0.047 m/s for PG. Another way of calculating the error in dynamic height is defining it as the error of the module of mean differences (Table 2). The mean difference is 0.05 dyn m, the standard deviation = 0.013 dyn m, and the standard error is ±0.0050 dyn m. By adding the error in the regression 0.027, the mean error in dynamic height for all sites is 0.032 dyn m.

2.2. Geostrophic Velocities and Transports

[14] From the dynamic height time series derived from the IES, it is possible to calculate surface geostrophic velocity time series. The average geostrophic velocity between two stations is given by

$$V_g = (10/f)(\delta D/\delta x), \tag{2}$$

where f is the Coriolis parameter, and δD is the difference of dynamic height between two stations separated by a distance δx. If it is assumed that there is no error in calculating the distance between stations, the error in geostrophic velocity ($\varepsilon(V_g)$) is the error of the differences in dynamic height, that is to say, the error in V_g is given by: $\varepsilon(V_g) = \sqrt{2}(10/f)\{\varepsilon(DH)/\Delta x\}$.

[15] The $\varepsilon(V_g)$ varies with the site not only because of the differences in errors for each dynamic height series but also because both f and Δx vary with the sites. The $\varepsilon(V_g)$ can be obtained in two different ways: (1) using the mean dynamic height error of the two series, the value of f at a mean latitude and the distance between the stations. Results are $\varepsilon\{V_g\,(14-16)\} = 0.008$ m/s; $\varepsilon\{V_g\,(6-17)\} = 0.028$ m/s; and $\varepsilon\{V_g$ (17-PG)$\} = 0.042$ m/s. (2) Using the mean error in dynamic height (0.032 dyn m). In this case $\varepsilon\{V_g\,(14-16)\} = 0.010$ m/s; $\varepsilon\{V_g\,(6-17)\} = 0.030$ m/s; $\varepsilon\{V_g$ (17-PG)$\} = 0.052$ m/s. In both cases, the errors are very similar.

[16] The relationship between the surface geostrophic velocity and the geostrophic transport in the upper 300 m is determined from the CTD stations collected during the cruises along the moored section as follows. We first assume that a linear relationship exists between the surface geostrophic velocity and the 0–300 m transport:

$$\mathrm{Tr} = k v_g\, \delta x\, \delta z, \tag{3}$$

where k is a constant to be determined, δx is the distance between stations, and $\delta z = 300$ m. From each of the CTD

Table 2. Comparison Between CTD and IES Dynamic Height (Figure 3)

IES/PG	Year	CTD (red), dyn m	IES/PG (black), dyn m	Difference, dyn m
IES 14	1999	0.570	0.568	0.007
	2000	0.560	0.527	0.003
IES 16	1999	0.808	0.805	0.003
	2000	0.788	0.791	−0.003
IES 17	1999	0.802	0.813	−0.011
	2000	0.766	0.755	0.010
PG	2000	0.730	0.695	0.035
Mean				0.015
Standard deviation				0.013
Standard error				±0.005

Comparison between the values of dynamic height obtained from CTD data (red circles in) collected during the NBCR cruises and the coincident values of dynamic height obtained from the travel time series.

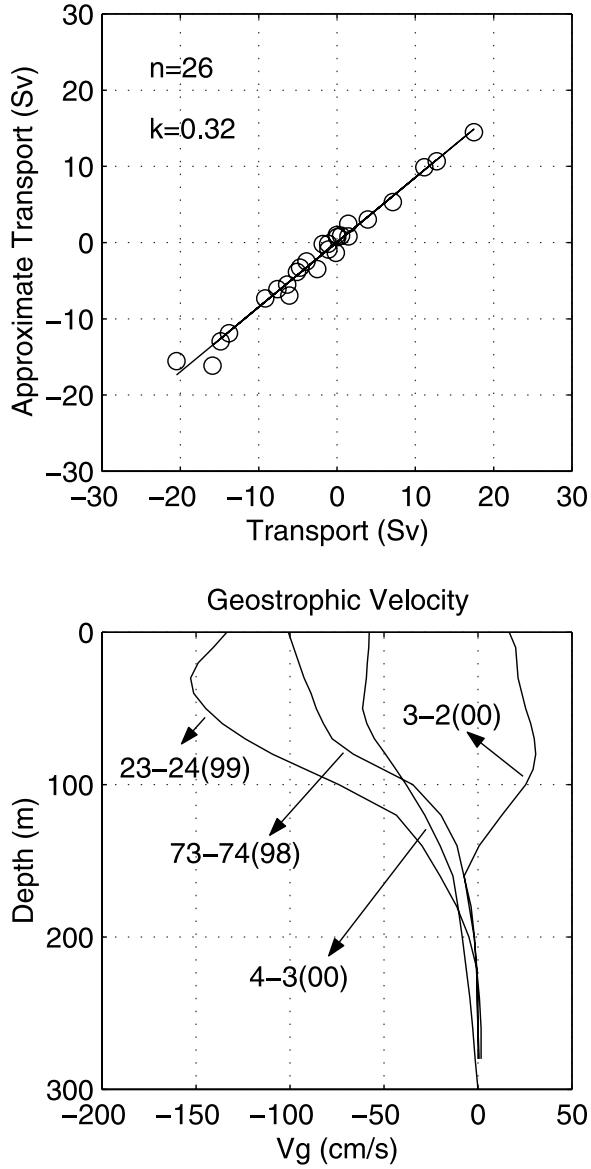

Figure 4. Results of the statistical analysis performed to determine the value of k (see text). (a) Regression between the transport calculated from the CTD data integrating from the surface to 300 m and the approximate transport obtained from the CTD data using the approximation $\mathrm{Tr} = kV_g\delta x\delta z$. (b) Examples of vertical profiles of the geostrophic velocities obtained between CTD station pairs and used to calculate the transports described above.

station pairs collected along the section, a value of the transport from the surface reference to 300 m was obtained as

$$Tr = \left\{ \int_0^{300\,\mathrm{m}} v_g(z)\delta x \right\} \delta z. \tag{4}$$

[17] These transports were regressed against the corresponding surface geostrophic velocities for the station pairs. The regression slope is $k = 0.32$, the error of the estimate $\varepsilon = \pm 0.024$, with $R^2 = 0.98$ (Figure 4).

[18] Examples of geostrophic profiles for the worst cases are shown in Figure 4b. The total error in the transports is a function of the error in k and the error in the geostrophic velocities. Following a procedure similar to the one used to obtain the errors in the geostrophic velocities, the errors in transport varies from ±1 Sv for the northernmost station to ±5 Sv for the southernmost one. The mean error in transport is ±2 Sv. Equation (3), with $k = 0.32$, is then applied to the time series of dynamic height from the IES to derive the geostrophic transports between the IES sites. The time series of geostrophic transport are given in Figure 5. It will be shown later that these derived transports agree well with independent estimates of the transport between the IES sites obtained from the available shipboard ADCP/LADCP sections.

2.2.1. Assessment of the Geostrophic Calculation

[19] The estimates obtained from the geostrophic relation are most accurate far from the equator and far from frictionally dominated boundaries. Consequently, the geostrophic transport estimates between IES 16 and 14 are likely to be the most accurate in this study. However, compared to snapshot, shipboard CTD measurements traditionally used in the geostrophic transport calculation, the pressure gauge and IES measurements used in this paper may be quite accurate because they were obtained from stationary bottom moorings and at high sampling rates, enabling considerable time averaging. While error analyses could be undertaken, the best assessment of the PG-IES transport estimates reported in this study is to compare them to the "snapshot" transport estimates derived from the four shipboard ADCP and LADCP velocity sections. In order to directly assess the accuracy of the PG-IES inferred transports, the integrated transports from the surface to 300 m are determined from the ADCP/LADCP station data and compared with the corresponding transports obtained from the moored instrument time series. Results of this comparison are listed in Table 3 and are shown graphically as diamonds on Figure 5. Also shown in Figure 5 (circles) are the values the geostrophic transports calculated from the CTD casts collected simultaneously to the LDCP. Table 3 lists the comparisons when transport from the two different methods can be obtained at the same time or, as in the case of November 1998, within only hours of each other. Listed in italic are the noncoincident values of transports. All of the transport estimates from CTD and ADCP/LADCP are shown in Figure 5. There are three times during the length of the experiment when accurate comparisons of the retroflected flow as measured from the ADCP/LADCP data and the moorings can be made: November 1998, March 1999, and February 2000. There is only one coincident comparison of the incoming NBC flow from the February 2000 cruise. A comparison for November 1998 was not possible due to the late deployment of the PG. There is no direct comparison available in March 1999 because the time series, due to the low-pass filtering and other data processing, begin after the stations were occupied. The one comparison in February 2000 is only with LADCP values because of poor shipboard ADCP data due to a malfunctioning gyrocompass during the first few days of the January–February 2000 cruise. For June 2000, comparisons

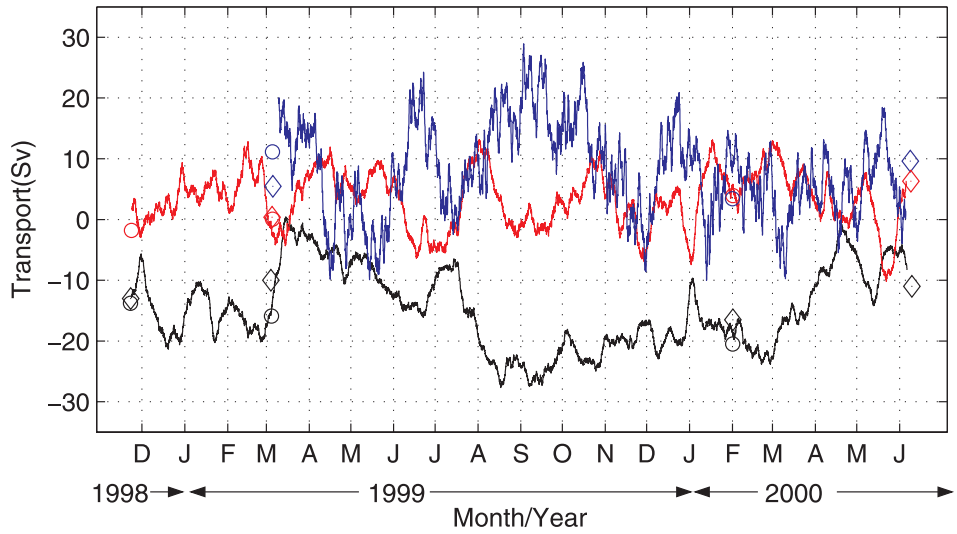

Figure 5. The time series of geostrophic velocities and transport between PG and IES 17 (blue), IES 17 and 16 (red), and IES 16 and 14 (black). Shown for comparison are transports calculated from the CTD casts (circles) and from the ADCP/LADCP (diamonds) when available.

are made with ADCP data only because no CTD/LADCP stations were taken during the recovery cruise. All the comparisons are within the error of ±2 Sv except for March 1999, in which the comparison is during the period of the most rapid change, 0–19 Sv in 10 days (Figure 5), during the entire 18-month deployment. In this case the difference is 5.4 Sv. It must be noted that at this particular time there is also a discrepancy between geostrophic transports from CTD stations (circles in Figure 5) and total velocities from ADCP/LADCP data (diamond in Figure 5). The ADCP and LADCP measure the total transport and they are in agreement with the transports calculated from geostrophy. Since these estimates are totally independent, it can be considered with a high level of confidence that all the previous assumptions are justified and that the transports obtained from the moored instruments are accurately measuring the flow of the upper 300 m within the above mentioned error bars. For completeness, the total northwestward NBC transport and the total retroflected transport is also calculated from the ADCP/LADCP sections obtained during the NBCR cruises and shown in Table 4. Note that the difference between these values and those previously reported in Table 3 is that in Table 4, total northeastward and southwestward transports are calculated while the values given in Table 3 are the values between fixed stations.

3. Volume Transports

[20] An analysis of historical data indicated that the dividing point between the northwestward NBC flow and the retroflected southeastward flow would be at the location where IES 16 was placed. For historic reference, see the work of *Bourles et al.* [1999a]. Consequently, most of the NBC flow transported northwestward should lie between IES 16 and the continental shelf (monitored by the pressure gauge and IES 17). The retroflected southeastward flow should be observed between IES 16 and 14 (the IES furthest offshore). The ADCP/LADCP sections occupied during the cruises indicate that IES 16 is indeed always between the high-velocity cores of the opposing flows. However, the location of these cores does change with time. For example, in November 1998 during Cruise 1, the core of the retroflected flow is at 4.5°N (Figure 2) at IES 16, whereas in March 1999 it is located near 5.5°N (not shown), which is between IES 14 and 16. During January 2000 and June 2000, the retroflected flow is also located near 5.5°N (not shown). This means that at times, the transports may be underestimated due to the spatial resolution. For the NBC inflow, the latitude of the core is at 2.5°N in November 1998, March 1999, and January 2000, and probably June 2000 (this recovery cruise did not fully resolve the nearshore portion of the section), that is to say between PG and IES 17. However, the front that divides the northwestward NBC flow from the southeastward retroflected flow varies. It is at 3.5°N in November 1998, 4.7°N in March 1999, 5.0°N in January 2000, and 4.2°N in June 2000, meandering between the gap between IES 17 and 16. This can be

Table 3. Comparison Between ADCP/LADCP and IES/PG Transports

NBC	LADCP, Sv	PG to IES 16	
November 1998	5.7	N/A	
March 1999	5.9	N/A	
February 2000	17.2	17.0 Sv	
May 2000	15.9	N/A	
Retroflected flow	ADCP/LADCP, Sv	IES 16 to 14, Sv	
November 1998	−13.0	−12.0	
March 1999	−10	−15.4	(slope)
February 2000	−16.5	−18.5	
May 2000	−11	N/A	

Transports estimated from the ADCP/LADCP data collected between the moored instruments (from PG to IES 16 and between IES 16 and 14) and the transport calculated from the dynamic height series at the corresponding locations.

Table 4. NBC Transports

Date	Transport, Sv	Measured With	Source
September 1995	22.3	ADCP	*Bourles et al.* [1999b]
April 1996	25.2	ADCP	
August 1989	17.1	ADCP	*Bourles et al.* [1999a]
January 1990	22.5	Pegasus	
September 1990	11.5	ADCP	
January 1991	16.1	ADCP	
June 1991	26.7	ADCP	
September 1991	25.7	ADCP	
November 1998	22.5	ADCP/LADCP	this paper
March 1999	5.8	ADCP/LADCP no shelf	
February 2000	17.2 Sv	LADCP no shelf	
Mean March 99 to June 2000	12.2	PG and IES	this paper

Comparison between transports obtained previously for the NBC at 44°W and calculated from the surface to the 26.75 isopycnals and those obtained in the present work at 47°W. Mean values are obtained from the time series collected with the moored instruments.

corroborated by the oscillations around zero observed in the time series of transport between IES 17 and 16 (Figure 5, red curve).

3.1. The NBC Transport

[21] The transport between the continental shelf and 3°N (Figure 5, PG to IES 17, blue line) is toward the northwestward for most of the observed period. The transport between 3° and 4°30′N (Figure 5, IES 17 to 16, red line) oscillates between northwestward and southeastward or it is close to zero, indicating the variability in the front's location with periods from 2 to 4 months. It is fair to assume that the lower bound of the NBC flow is the sum of the transport between the two stations closest to the coast (PG and 17) plus the positive values of the transport between IES 16 and 17. The results of these calculations are shown in Figures 6 and 7 that shows the total NBC transport (blue line) and the total retroflected flow (red line) as monitored by the IES and the PG.

[22] The total NBC transport (Figure 6) is toward the northwest for most of the 15-month record, as expected. The mean of the northwestward flow during the entire period of observations is 12.1 ± 2 Sv, with a maximum of 31.8 ± 2 Sv around 15 October 1999 and a minimum of −8.6 ± 2 Sv around 1 December 1999. However, there is considerable high-frequency variability throughout the record such that the transports fluctuate on the order of at least 10 Sv to more than 20 Sv in any one month. Nonetheless, the March, June, and August–October 1999 time periods reveal the highest mean transports (on the order of 20 Sv), the December 1999 to June 2000 time period reveals moderate mean transports (on the order of 10 Sv), and the April–May, July, and November 1999 time periods reveal lowest mean transports (on the order of 5 Sv). During the same time periods that the record reveals low northwestward transports, or even southeastward transports (negative values), the full array of moored instruments from the experiment reveals that the NBC retroflection is at, or southeast of approximately 47°W, 2.5°N [*Garzoli et al.*, 2003]. Consequently, when the NBC flow is a minimum at 47°W, 2.5°N, the retroflection is probably located southeast of this location and its transport would not necessarily be low if measured at a location further southeast. Excluding the time periods when the retroflection is southeast of 47°W, 2.5°N, the mean northwestward NBC transport is 18 ± 2 Sv. This value compares well with previous estimates from ADCP/LADCP

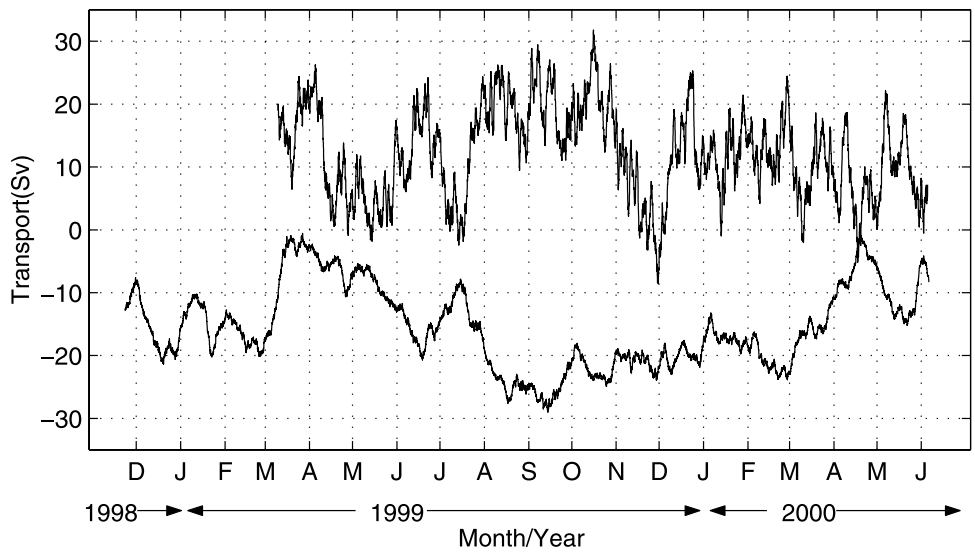

Figure 6. Time series of transport of the NBC (positive curve) and the retroflected flow (negative flow).

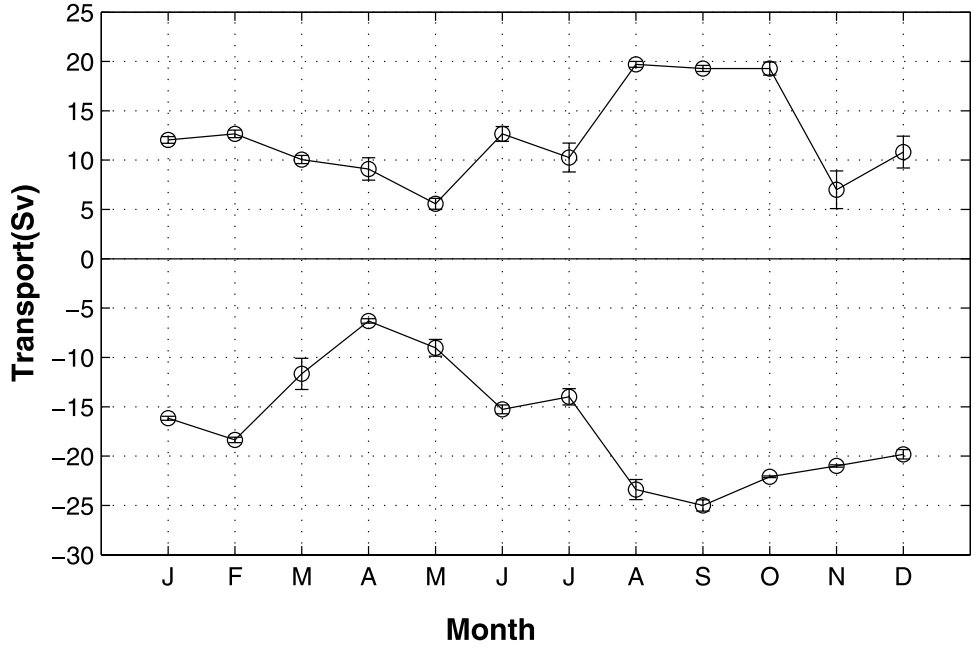

Figure 7. Annual cycle of the NBC obtained using the same smoothing procedure that *Johns et al.* [1998] used and of the retroflected flow. Vertical lines indicate the standard deviation of the mean values obtained from the 30-day running mean values of the transport series.

data of the NBC. These estimates are summarized in Table 4, and their average is 20.9 Sv. All values from the work of *Bourles et al.* [1999a, 1999b] are obtained at 44°W and calculated from the surface to the 26.75 isopycnal. However, it must be noted that the historical observations that average to 20.9 Sv are mostly collected during summer and fall when the NBC tends to be strongest [*Johns et al.*, 1998]. Also, note that the transports derived from the moored instruments presented here do not include the transport on the shelf. The shelf transport estimate can be estimated as an average of all previous observations [2.8 ± 1.3 Sv, *Johns et al.*, 1998] plus our shelf estimate from November 1998 (3.3 Sv). The result is 2.9 Sv. If this value is added to the mean northwest transport during the entire period of observations, the average NBC transport is 15.1 Sv. For the period of time when the retroflection is southeast of 44°W, the mean NBC transport is 21.1 Sv. This value should also be added to the ADCP/LADCP transports obtained for March 1999 and February 2000.

[23] An important fact to note is that the cruise observations listed in Table 4 have a large range of values, from 5.8 to 26.7 Sv, consistent with the large variability observed by the IES/PG array and shown in Figure 6. This variability is not only seasonal. Estimates obtained in different years but in the same month, for example, September, vary from 11.5 to 25.7 Sv. Consequently, values from the transport of the NBC derived from single cruises should be considered in the context of this high intraseasonal and interannual variability.

[24] *Johns et al.* [1998] used data collected over a 1-year period with an array of current meters between the Brazilian continental slope and near 45°W, 4°N to study the seasonal cycle of the NBC. From this study it was concluded that the NBC has a large annual cycle at this latitude, ranging from a maximum transport of 36 Sv in July–August to a minimum of 13 Sv in April–May. This transport cycle was explained partially by linear wind-driven Sverdrup theory. However, it was shown that the mean transport of the NBC is 15 Sv larger than can be explained by wind forcing only, indicating a strong thermohaline component. The results shown in Figure 6 do not indicate an obvious seasonal cycle that follows the curl of the winds which would lead to a minimum transport during May, increasing rapidly and steadily to a maximum value during August and a slow decrease again to May. It must be noted that *Johns et al.*'s [1998] results were obtained by averaging all the monthly means together into one annual cycle after the data were passed through 2-day and 30-day consecutive running mean filters. If the same treatment is applied to the PG-IES transport time series (Figure 6), the result (Figure 7) exposes features similar to *Johns et al.* [1998]: the mean annual NBC transport time series indicates an average minimum in May and average maximum values in August, September, and October, with a secondary maximum in February. Note that while the NBC curve in Figure 7 is referred to as a mean annual time series, only 15 months of data are used to construct it with just the 3-month period, March–May, overlapping twice. The main difference is that instead of a steady increase in the values from May through August, a secondary minimum is observed in July. The analysis of the curl of the wind stress at 47°W, 4°N obtained from the European Centre for Medium-Range Weather Forecasts' (ECMWF) winds for the period of the observations (not shown) does not show significant differences with climatology nor with the wind data used by *Johns et al.* [1998] that could explain this secondary minimum of July. Therefore the differences may be due to difference in location along the western boundary or due to a small period of time during which the observations overlap twice.

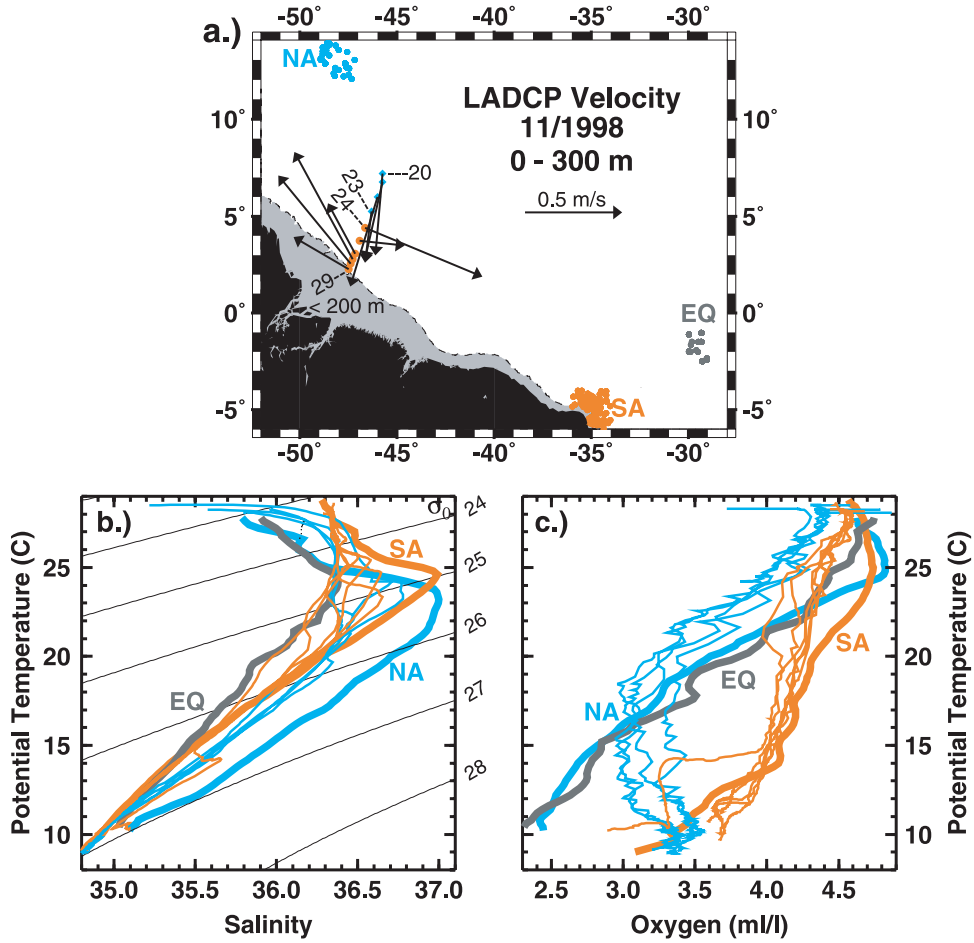

Figure 8. (a) Map showing the averaged 0–300 m, LADCP velocities between the PG and IES 14 for November 1998. In addition, the locations of the National Oceanographic Data Center historical stations used to define the North Atlantic (NA, in blue), South Atlantic (SA, in orange), and equatorial (EQ, in gray) water masses are shown by solid circles. (b) Potential temperature-salinity plot of the averaged NA (blue), SA (orange), and EQ (gray), 0–300 m, historical data (thick lines). In addition, the 0–300 m, station data obtained during the November 1998 cruise is shown, color coded by water mass origin: stations 20–23 of North Atlantic origin (thin blue lines) and stations 24–29 of South Atlantic origin (thin orange lines). (c) The same as in Figure 8b but for potential temperature-oxygen.

[25] Another difference between the annual cycle of the NBC shown in Figure 7 and results from *Johns et al.* [1998] is in the intensity of the flow. In the work of *Johns et al.* [1998] the mean maximum observed NBC flow for the month of August is 35 Sv, while the one observed in the present study is in the mean 20 Sv. The results suggest a transport growth of approximately 10 Sv in the NBC between the location of our moored section (~2°N) and the *Johns et al.* [1998] location (4°N). Some support for this conclusion is found in models (M. Jochem, personal communication, 2003) which indicate a similar increase in the NBC transport of about 10 Sv between these two locations.

3.2. The Retroflected Transport

[26] It is reasonable to assume that the lower bound of the retroflected flow is the sum of the transport between IES 16 and 14 plus the negative portions of the transport between IES 17 and 16. The results of adding these values are shown in Figure 6. The retroflected flow is always toward the southeast, as expected. The mean of the southeast flow is 16 ± 2 Sv, with a minimum value of 0 ± 2 Sv and a maximum of 28 ± 2 Sv. The southeast flow reaches its maximum value during September 1999, near the time when the climatological North Equatorial Countercurrent (NECC) reaches its maximum strength in October, and it is minimum during March–April 1999 and April 2000 when the climatological NECC reverses or is not present in the basin [*Garzoli and Katz*, 1983; *Garzoli*, 1992]. The mean value of 16 Sv obtained for the retroflection transport from our time series is lower than the 21.7-Sv mean of the values obtained from ADCP/LADCP sections in the literature as well as the 20.5-Sv estimate obtained when we average the three ADCP/LADCP values obtained in the present work (Table 5). This may be due to the fact that five out of the nine estimates are during the August–November maximum seasonal flow. If the mean of the transport time series (Figure 6) between August and November 1999 is calculated, the value obtained is 22 Sv, exactly the same as the mean of the five direct estimates during the period of high transport. There is a large interannual and seasonal variabil-

Table 5. Retroflected Flow

Date	Transport, Sv	Measured With	Source
September 1995	28.8	ADCP	*Bourles et al.* [1999b]
April 1996	27.3	ADCP	
August 1989	17.6	ADCP	*Bourles et al.* [1999a]
September 1990	18.9	ADCP	
June 1991	17.0	ADCP	
September 1991	20.6	ADCP	
November 1998	25.6	ADCP/LADCP	this paper
March 1999	12.4	ADCP/LADCP	
February 2000	16.5	ADCP/LADCP	
Mean (November 1998 to June 2000)	16.0 Sv	PG and IES	this paper

Comparison between transports obtained previously for the retroflected flow at 44°W and those obtained in the present work. The values for the dates of the cruises correspond to values obtained from the LADCP/ADCP observations. Mean values are obtained from the time series collected with the moored instruments.

ity in the previously observed transports (Table 5) [*Bourles et al.*, 1999a, 1999b]. The three ADCP/LADCP realizations obtained during the NBCR cruises match well the values obtained with the moored instruments.

[27] An analysis of Figure 6 indicates the possibility of an annual cycle: in March 1999 the southeastward flow rapidly diminishes to zero, then steadily increases from April through August, when it remains high until March 2000, when it again diminishes to zero. These results are very similar to those obtained by *Garzoli* [1992] from two inverted echo sounders deployed at 7°N, 44°W and 3°N, 44°W. The mean annual cycle of the retroflected flow is shown in Figure 7. Note that while the retroflected flow curve in Figure 7 is referred to as a mean annual time series, only 18 months of data are used to construct it with just the 6-month period, December–May, overlapping twice.

[28] There is a difference between the mean incoming (northwestward) flow (12 Sv) and the outgoing (southeastward) flow (−16 Sv). If we add the shelf flow (3 Sv), the total incoming flow (∼15 Sv) is balanced by the retroflected flow (∼16 Sv) within the limits of the errors. However, considering the mean of the incoming flow (shelf included) and the mean of the retroflected flow during the period of time when the NECC is fully present in the Atlantic basin west of 40°W [July–December, *Garzoli and Katz*, 1983], the difference between the total incoming (16 Sv) and the retroflected flow (23 Sv) is 7 Sv. This is an indication that when the NECC is fully formed there is an additional flow between IES 16 and 14. This flow is of North Atlantic origin and may be associated with the North Equatorial Current (NEC). This has been previously noted from hydrographic observations [e.g., *Bourles et al.*, 1999a]. In the work of *Bourles et al.* [1999a], a mean "deficit" of 7 Sv between incoming and retroflected flow at 44°W is observed and it is concluded that the NECC is composed of waters from both hemispheres. This is confirmed in the NBCR observations. For example, in November 1998, the combined ADCP/LADCP section yields a 3.4-Sv shelf flow, 19.1-Sv NBC flow, and −25.6-Sv retroflected flow. The difference between the NBC flow and the retroflected flow is −6.5 Sv. A similar result is obtained in March 1999, with the difference between a 5.8-Sv NBC flow and a −12.4-Sv retroflected flow of −6.6 Sv. In contrast, during February 2000, the NBC flow is 17.7 Sv and the retroflected flow is −16.5 Sv, with a difference of 1.2 Sv.

[29] To determine the difference in the origins of the water masses of these flows, the water properties for the different stations are examined [e.g., *Bourles et al.*, 1999a]. In addition, they are compared to historical station data obtained from the National Oceanographic Data Center from the regions that display characteristics of the source water masses. An example is shown for November 1998 (Figure 8). In this example, the 0–300 m averaged LADCP velocities (Figure 8a) clearly show the northwestward NBC flow (stations 26–29) and the southeastward retroflected flow (stations 24–25). By examining Figure 8c, the NBC and retroflected flow (stations 24–29, thin orange lines) are clearly of South Atlantic origin (thick orange line), as all the oxygen values are relatively high, and similar to the historical oxygen values observed further south at the origin of the NBC. Further north (stations 20–23), the averaged LADCP velocities indicate a southward flow feeding into the southeastern retroflected flow (Figure 8a). These northernmost stations (thin blue lines) are clearly not South Atlantic in origin (thick orange line) because all their oxygen values are relatively low compared to the values observed in the South Atlantic water masses (Figure 8c). Because a South Atlantic origin is ruled out, stations 20–23 can now be identified as either being from the North Atlantic or of equatorial origin on the basis of their salinity values in comparison to the historical values (Figure 8b). It is likely that stations 20–23 (thin blue lines) are of northern origin (thick blue line) because they are all saltier than the historical equatorial curve (thick gray line). Consequently, it is possible to confirm that the excess in the retroflected flow is due to North Atlantic water joining the retroflected flow from the South Atlantic. The combination of both flows constitutes the NECC. According to *Garzoli and Katz* [1983], during April and May at 47°W the NECC is not observed. In the center of the tropical Atlantic basin, this reversal of the NECC is directly caused by the reversal of the trade winds through the combined mechanism of local Ekman pumping and the divergence of the geostrophic currents [*Garzoli and Katz*, 1983]. The agreement is no longer valid west of 45°W. This disagreement could be due to the fact that during the period of time when the NECC is stronger it has two main contributors: waters from the South Atlantic carried by the NBC and retroflected and water from the North carried by the NEC.

3.3. The NBC Transport and the Latitude of Penetration

[30] As was mentioned in section 1, *Garzoli et al.* [2003] analyzed synoptic maps of dynamic height produced from

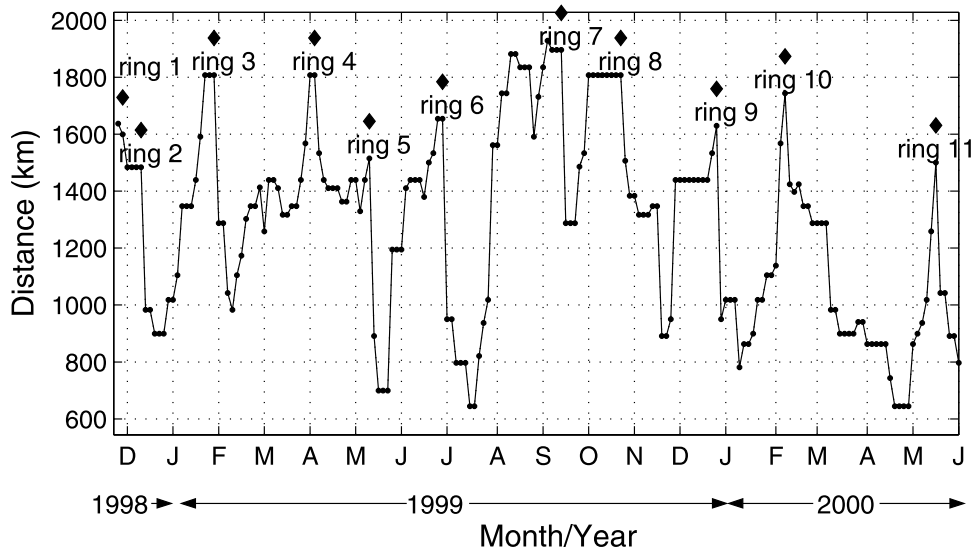

Figure 9. Latitude of the northwestward penetration of the NBC measured as the distance of the northernmost point of the retroflection and an arbitrary point in space (0°N, 42°W) [adapted from *Garzoli et al.*, 2003].

the data collected with the IES array. One of the results of this analysis was a time series that indicated the latitude of penetration of the NBC retroflection. The latitude of penetration was determined as the distance between a point near the western boundary on the equator (0°N, 42°W) and the northernmost extension of the NBC. The results of this work are reproduced in Figure 9. The way this figure should be interpreted is as follows [see *Garzoli et al.*, 2003]: during the northward motion of the NBC, the curve represents the actual northwestward motion of the retroflection, which advances at typical speeds of 30 km/d. Once the retroflection closes upon itself and a ring is shed, the curve shows the location of the new position of the retroflection, now to the southeast of the newly formed ring. Therefore the descending part of the curve does not represent a continuous retraction of the retroflection. The southward motion is a resetting index and cannot be inferred from the figure. As the ring separates, the retroflection forms again further south. A ring with a diameter ranging between 300 and 400 km is located between the previous location and the new one [*Garzoli et al.*, 2003].

[31] The incoming NBC flow is compared to the latitude of penetration of the retroflection in Figure 10. For the purpose of comparison, both series are plotted as anomalies with respect to the mean value of each series. The transport series are subsampled to 3-day means to directly compare with the distance series (created from frames obtained at a 3-day interval). Differences in sampling explain some

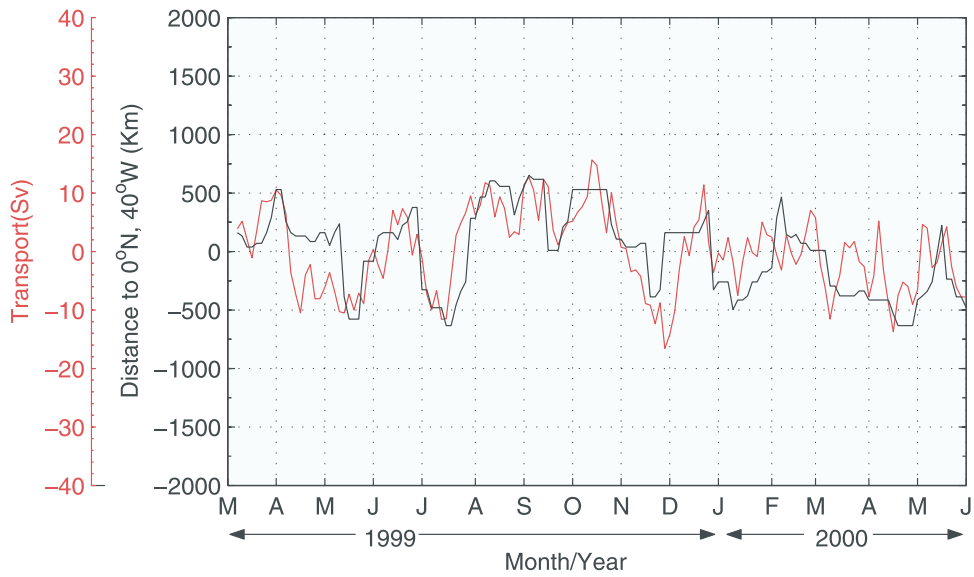

Figure 10. Comparison between the variability of the latitude of the retroflection and the variability of the NBC transport.

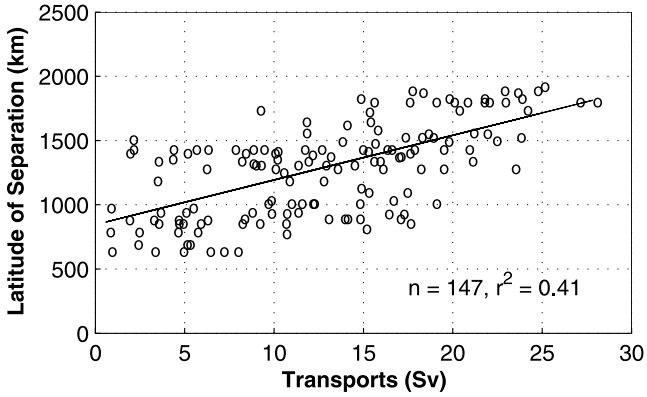

Figure 11. Relation between the latitude of separation of the NBC from the coast and the volume transport. The line is the best fit to the data.

differences with transport shown in Figures 5 and 6. There is an apparent correlation between the two series in that when the NBC transport is high (low), the retroflection occurs further northwest (southeast). Another way of looking at this correlation is presented in Figure 11 that shows a noisy but positive correlation between the NBC and latitude of penetration in which the stronger the current, the further northwest the retroflection tends to occur. The coefficient of correlation between the two series is $r = 0.60$, a value that may not be significant but the tendency is clear. As shown by *Garzoli et al.* [2003] and *Fratantoni and Glickson* [2002], in general, a ring is shed when the retroflection retracts from a maximum northwestward position. Here it is concluded that in addition the NBC flow is also at a maximum just before the NBC reaches its northernmost extension and a ring is shed. The coincidence of maximum current transport and ring shedding is similar to observations in other western boundary currents. For example, a similar phenomenon is found at the retroflection of the Agulhas Current in the South Atlantic [*Goni et al.*, 1997; *Garzoli and Goni*, 2000]. Estimates of Agulhas transport obtained from altimeter data indicated that a peak in the transport was followed by the shedding of a ring.

[32] A possible explanation of the observed relation between ring shedding and transport is associated with the process of ring shedding itself. Previous observations have shown that anticyclonic eddy features exist in the NBC upstream of the retroflection [*Johns et al.*, 1998], which may propagate downstream within the NBC and serve as a catalyst for NBC ring shedding. *Johns et al.* [1998] described these features as being "embedded in, or adjacent to, the NBC," with downstream propagation speeds of about 8 km/d. If we assume this is the case, these features should pass though our inflow section (PG to IES 17) at some time before they reach the retroflection. Their effect on the transport would be to enhance the northwestward transport of the NBC near the coast and increase the southeastward retroflected flow farther offshore. It can be seen in Figure 6 that several of the NBC transport events that correspond to increased penetration of the retroflection and ring generation have this character: an increase in both transport of the NBC and the retroflected flow. However, one would expect these transport events to lead the pinch-off of rings by the time it takes these eddy features to propagate from the inlet section to the latitude of the retroflection, which would be on the order of a month. This in fact does not appear to be the case, as our results suggest transport fluctuations that are nearly in phase with the NBC penetration and ring shedding events. The degree of correlation between the transport, NBC penetration, and ring shedding time sequences, however, is not high enough to rule out such a time lag. Thus such a mechanism seems a plausible but not obvious explanation for the observed relationships. Alternatively, a mechanism involving Rossby waves propagating into the western boundary and reflecting from the boundary could cause the observed behavior of the transport fluctuations and NBC ring shedding. Such a process has been proposed recently by *Jochum and Malanotte-Rizzoli* [2003], who found in a model study that baroclinic Rossby waves generated from an instability of the NECC propagate westward to the retroflection and induce NBC ring shedding. The extent to which this or other processes are consistent with the observed correlation among the retroflection penetration, upstream transport variability, and ring shedding is a topic that deserves further investigation.

4. Summary

[33] In this paper, it was shown that a combination of IES and a pressure gauge was an efficient method to monitor the upper ocean transport of the NEC and the retroflected flow. These measurements, calibrated with other in situ observations, provided an 18-month time series of integrated transports in the region. The mean NBC flow observed during the entire period of the observations (May 1999 to June 2000) was 12.1 ± 2 Sv, with a maximum value of 32 ± 2 Sv observed in September 1999 and a minimum of -5 ± 2 Sv observed during the month of May 1999. Excluding the periods of time when the retroflection of the NBC occurs southeast of 47°W (i.e., south of the line of instruments) the mean NBC transport is 18 ± 2 Sv. This value compares well with previous estimates from ADCP/LADCP data of the NBC at 44°W. The retroflected flow was monitored at the same latitudes and for a longer period of time, (November 1998 to June 2000). The mean southeast flow was 16 ± 2 Sv, with a minimum value of 0 ± 2 Sv and a maximum of 28 ± 2 Sv. This southeast flow reaches its maximum value during September 1999, near the time when the climatological NECC reaches its maximum strength in October and it is weakest during March–April 1999 and April 2000 when the climatological NECC reverses or is not present in the basin. The difference between the NBC flow and the retroflected flow during the period of time when the NECC is fully formed is -7 Sv. The CTD-O_2 data were analyzed to determine the origins of the surplus flow. This analysis indicated that the excess in the retroflected flow is due to North Atlantic water joining the retroflected flow from the South Atlantic. The combination of both flows constitutes the NECC. Finally, the time series of the NBC transport are compared with the westward penetration of the NBC. The latter was previously determined from the analysis of synoptic maps of dynamic height obtained from a larger array of IES. It is concluded that there is a direct relationship between the latitude of penetration and the intensity of

the NBC. When the NBC transport is maximum, the current reaches its maximum latitude of penetration and a ring is shed. The whole system retracts and starts moving northeastward again as the transport of the NBC starts to increase again.

[34] **Acknowledgments.** The authors are indebted to the crew of the R/V *Seward Johnson* for their support during the four cruises. The IES were prepared for deployment, deployed, and recovered by David Bitterman. Roberta Lusic prepared the manuscript for electronic submission. Support for this project was provided by NSF grant OCE-97-32389 and by NOAA AOML. Ship time for the cruises was funded by NSF and NOAA/OAR.

References

Bourles, B., R. L. Molinari, E. Johns, W. D. Wilson, and K. D. Leaman (1999a), Upper layer current in the western tropical North Atlantic, *J. Geophys. Res.*, *104*, 1361–1375.

Bourles, B., Y. Gouriou, and R. Chuchla (1999b), On the circulation in the upper layer of the western equatorial Atlantic, *J. Geophys. Res.*, *104*, 21,151–21,170.

Didden, N., and F. Schott (1993), Eddies in the North Brazil Current retroflection region observed by geosat altimetry, *J. Geophys. Res.*, *98*, 20,121–20,131.

Egbert, G. D., A. F. Bennett, and M. G. G. Foreman (1994), TOPEX/POSEIDON tides estimated using a global inverse model, *J. Geophys. Res.*, *99*, 24,809–24,820.

Fratantoni, D. M., and D. A. Glickson (2002), North Brazil Current Ring generation and evolution observed with SeaWiFS, *J. Phys. Oceanogr.*, *32*, 1058–1074.

Fratantoni, D. M., W. E. Johns, T. L. Townsend, and H. E. Hurlburt (2000), Low-latitude circulation and mass transport pathways in a model of the tropical Atlantic Ocean, *J. Phys. Oceanogr.*, *8*, 1944–1966.

Garzoli, S. L. (1984), Modes of variability of the 1983: Thermocline signal, *Geophys. Res. Lett.*, *11*, 741–744.

Garzoli, S. L. (1992), The Atlantic North Equatorial Countercurrent: Models and observations, *J. Geophys. Res.*, *97*, 17,931–17,946.

Garzoli, S. L., and Z. Garraffo (1989), Transports, frontal motions and eddies at the Brazil-Malvinas Currents confluence, *Deep Sea Res., Part A*, *36*, 681–703.

Garzoli, S. L., and G. J. Goni (2000), Combining altimeter observations and oceanographic data for ocean circulation studies, in *Satellites, Oceanography and Society*, chap. 5, edited by D. Halpern, pp. 79–97, Elsevier Sci., New York.

Garzoli, S. L., and A. L. Gordon (1996), Origins and variability of the Benguela Current, *J. Geophys. Res.*, *101*, 879–906.

Garzoli, S. L., and E. Katz (1983), The forced annual reversal of the Atlantic North Equatorial Countercurrent, *J. Phys. Oceanogr.*, *13*, 2082–2090.

Garzoli, S. L., A. L. Gordon, V. Kamenkovich, S. Pillsbury, and C. Duncombe-Rae (1996), Variability and sources of the South Eastern Atlantic circulation, *J. Mar. Res.*, *54*, 1039–1071.

Garzoli, S. L., A. Ffield, and Q. Yao (2003), NBC retroflection and rings, in *Interhemispheric Water Exchange in the Atlantic Ocean*, *Elsevier Oceanogr. Ser.*, vol. 68, edited by G. Goni, and P. Malanotte-Rizzoli, pp. 357–374, Elsevier Sci., New York.

Goni, G., and W. E. Johns (2001), A census of North Brazil Current Rings observed from TOPEX/POSEIDON altimetry: 1992–1998, *Geophys. Res. Lett.*, *28*, 1–4.

Goni, G. J., and W. Johns (2003), Study of North Brazil Current Rings using altimetry data, in *Interhemispheric Water Exchange in the Atlantic Ocean*, *Elsevier Oceanogr. Ser.*, vol. 68, edited by G. Goni and P. Malanotte-Rizzoli, Elsevier Sci., New York.

Goni, G., S. L. Garzoli, A. Roubicek, D. Olson, and O. Brown (1997), Agulhas rings dynamics from TOPEX/POSEIDON satellite altimeter data, *J. Mar. Res.*, *55*, 861–883.

Jochum, M., and P. Malanotte-Rizzoli (2003), On the generation of North Brazil Current Rings, *J. Mar. Res.*, *61/2*, 147–162.

Johns, W. E., T. N. Lee, F. A. Schott, R. J. Zantop, and R. H. Evans (1990), The North Brazil Current retroflection: Seasonal structure and eddy variability, *J. Geophys. Res.*, *95*, 22,103–22,120.

Johns, W. E., T. N. Lee, R. C. Beardsley, J. Candela, R. Limeburner, and B. Castro (1998), Annual cycle and variability of the North Brazil Current, *J. Phys. Oceanogr.*, *28*, 103–128.

Johns, W. E., R. J. Zantopp, and G. J. Goni (2003), Cross-gyre transport by North Brazil Current Rings, in *Interhemispheric Water Exchange in the Atlantic Ocean*, *Elsevier Oceanogr. Ser.*, vol. 68, edited by Malanotte-Rizzoli and Goni, Elsevier Sci., New York.

Richardson, P. L., and S. L. Garzoli (2003), Characteristics of intermediate water flow in the Benguela Current as measured with RAFOS floats, *Deep Sea Res., Part II*, *50*(1), 87–118.

Richardson, P. L., G. E. Hufford, R. Limeburner, and W. S. Brown (1994), North Brazil Current RetSwaroflection eddie, *J. Geophys. Res.*, *99*, 5081–5093.

Schott, F. A., L. Stramma, and J. Fischer (1995), The warm water inflow into the western tropical Atlantic boundary regime, 1994, *J. Geophys. Res.*, *400*, 24,745–24,760.

Schott, F. A., J. Fischer, and L. Stramma (1998), Transports and pathways of the upper-layer circulation in the western tropical Atlantic, *J. Phys. Oceanogr.*, *28*, 1904–1928.

Stramma, L., J. Fischer, and J. Reppin (1995), The North Brazil Undercurrent, *Deep Sea Res., Part I*, *42*, 773–795.

Watts, D., and W. Johns (1982), Gulf stream meanders: Observations on propagation and growth, *J. Geophys. Res.*, *87*, 9467–9476.

A. Ffield, Lamont-Doherty Earth Observatory of Columbia University, Palisades, NY 10964, USA.

S. L. Garzoli, Atlantic Oceanographic and Meteorological Laboratory, National Oceanic and Atmospheric Administration, 4301 Rickenbacker Causeway, Miami, FL 33149, USA. (garzoli@aoml.noaa.gov)

W. E. Johns, Rosenstiel School of Marine and Atmospheric Sciences, University of Miami, Miami, FL 33149, USA.

Q. Yao, Cooperative Institute for Marine and Atmospheric Studies, Miami, FL 33149, USA.